Available online at www.sciencedirect.com
ScienceDirect
Journal of the European Ceramic Society 26 (2006) 3221–3231
www.elsevier.com/locate/jeurceramsoc

The current detour effect observed on materials with random microstucture: experimental evidence from $Li_{3x}La_{2/3-x}TiO_3$ studied by impedance spectroscopy

Murugesan Vijayakumar, Odile Bohnke *

Institut de Recherche en Ingénierie Moléculaire et Matériaux Fonctionnels (FR 2575 CNRS), Laboratoire des Oxydes et Fluorures (UMR 6010 CNRS), Université du Maine, Avenue Olivier Messiaen, 72085 Le Mans Cedex 9, France

Received 20 April 2005; received in revised form 27 September 2005; accepted 30 September 2005
Available online 14 November 2005

Abstract

Impedance spectroscopy (IS) has been used to study the influence on the low frequency part of the impedance diagrams of the microstructure of a fast ionic conductor, $Li_{3x}La_{2/3-x}TiO_3$ with $x = 0.10$ (named hereafter LLTO). This oxide has been synthesised by sol–gel method. After synthesis, the powder of LLTO displays a large distribution of grain size and agglomerates. The grain size distribution and the porosity of the ceramic have been changed by heat-treatment from 600 °C to 1200 °C in air. The impedance spectra of these ceramics, recorded at different temperatures from room temperature (RT) to 400 °C, show a low-frequency depressed arc, which is characteristic of the grain boundary response of the ceramic. Its shape depends strongly on the heat-treatment of the ceramic, and therefore, on its microstructure. It is a simple arc when the pellet is well sintered but becomes very complex for non-sintered ceramics with high resistive grain boundary and pores. The observed "fish" shape indicates the presence of current "detours effect" in the material. This effect means that current detours around blocking grain boundary and/or pores occur to lower the impedance. Consequently, the brick layer model (BLM), which assumes an ideal microstructure, and then no current "detours effect", can not be used to analyse these impedance data.

Keywords: Impedance spectroscopy; Ionic conductivity; Grain boundaries; (Li, La)TiO_3

1. Introduction

Transport property of polycrystalline solid electrolytes is generally characterised by the bulk conductivity or intra-grain ionic transport. However, grain boundaries property is also very important as soon as the electrolyte is used in an electrochemical device, such as batteries, sensors or electrochromic windows. In such devices, the overall conductivity of the ceramic electrolyte should be as high as possible and then the additional resistances caused by grain boundary effects are unwelcome. Therefore, the control of grain boundary electrical properties has attracted much attention. The grain boundary electrical property is often linked to the microstructure of the ceramic and then the synthesis and the sintering procedures used to prepare the ceramic is of great importance. Impedance spectroscopy (IS) is an important tool to investigate the electrical properties of polycrystalline electrolytes because this technique allows to separate the ionic motion into the grains from the one into the grain boundaries, as soon as the rates of these processes are sufficiently different. When it is the case, the complex impedance data, displayed in a Nyquist plane, usually result in two or several more-or-less separated semicircles.[1]

To analyse the impedance spectra and to interpret the raw data in terms of bulk and grain boundaries impedance, a model is necessary. The role of the model is then to provide a hypothetical microstructure of the ceramic for which the overall complex impedance or conductivity can be calculated. In general, from the model of the microstructure, an electrical equivalent circuit representation can be derived. This is a convenient way, since the electrical circuit parameters can be estimated from the IS data. As pointed out by Bonanos et al.,[1] a number of electrical models may give rise to the same impedance diagrams but all

* Corresponding author. Tel.: +33 2 4383 3354; fax: +33 2 4383 3506.
E-mail address: odile.bohnke@univ-lemans.fr (O. Bohnke).

0955-2219/$ – see front matter © 2005 Elsevier Ltd. All rights reserved.
doi:10.1016/j.jeurceramsoc.2005.09.107

the models do not predict the same values for the conductive and capacitive components, leading to a possible misinterpretation of the real electrical properties of the material under study if a non-realistic electrical model is used. The earliest simple series model, originally proposed by Maxwell to describe the electrical properties of a two-phase mixtures,[2] has been extensively used since the first work of Bauerle that demonstrated the usefulness of the complex admittance approach in solid electrolyte studies.[3] Now, the brick layer model (BLM), suggested by Beekmans et al.[4] has been extensively used to analyse impedance spectra in ceramics with highly resistive grain boundaries.[5–8] This model takes into account an ideal microstructure of the ceramic and assumes a regular, cubic and isotropic grains of the same size. The contact between grains is flat and display uniform properties resulting in a current flow, which is one-dimensional from one electrode to the other. It has to be emphasised that in this model, the current density in the sample is totally homogeneous, resulting from a homogeneous potential distribution. This model can be described by an equivalent electrical circuit consisting of two serial RC elements, one being generally related to the bulk and the other to the grain boundaries of the material.

However, this ideal microstructure is far away from the microstructure of real systems. A real ceramic neither displays a constant size grain nor a uniform grain boundary property. Consequently, such real microstructures, differing from the BLM, can cause inhomogeneous potential distribution, and therefore, can lead to a non-homogeneous current flow. Recent studies reported by Fleig et al.[9–13] clearly showed how deviations from the idealised model, and particularly from homogeneous current density, influence the overall impedance for high resistive grain boundaries. They proposed a new concept of current "detours" to explain the behaviour of the low-frequency semicircle observed in the impedance spectra of inhomogeneous grain size ceramics. In this paper, this concept has been successfully incorporated to explain the electrical property of the non-homogeneous microstructured fast lithium conductive ceramic $Li_{3x}La_{2/3-x}TiO_3$ with $x = 0.10$.

Recently, Bohnké et al. reported the use of these ceramics as ion-selective electrode for pH detection.[14–16] They particularly showed the influence on the pH detection of the grinding of the powder and of the sintering temperature used for the pellets preparation. These results spurred an interest to study the effect of sintering temperature which yields the suitable grain boundary microstructure of LLTO to apply as successful pH sensors. The aim of this paper is then to study the electrical property of sintered pellets of LLTO obtained from a powder made of a large grain size distribution, with small as well as large grains with agglomerations of grains. Such a large distribution has been achieved by synthesis of the powder by polymerizable precursor method which yields the highly pure LLTO with inhomogeneous distribution of grain sizes.[17] The Fleig's concept of current "detour" will be applied to these ceramics to explain the shape of the impedance data. In order to avoid any confusion about terminology, we will use the term *total conductivity* when ionic plus electronic conductivity are concerned and the term *overall conductivity* to designate bulk plus grain boundary conductivity. It has to be recalled that impedance data is unable to separate ionic and electronic conductivity and then give, for each frequency, the total conductivity. On the other hand, bulk and grain boundary resistance can be separated by this technique.

2. Experimental

The $Li_{0.3}La_{0.56}TiO_3$ powder is synthesised by polymerizable precursor method and the detailed procedure has been previously reported.[17] The pellets are prepared by cold isostatically pressing the powder with a pressure of 5 MPa.

The dilatometry studies are carried out with a Setsys Evolution TMA equipment from Setaram. The dilatometry measurements are carried out on constant air flow with heating rate of $5\,^{\circ}C\,min^{-1}$ in the temperature range from room temperature (RT) to 1350 °C. Previous measurements in N_2 atmosphere (an inert gas with low pressure of oxygen) lead to the reduction of titanium, due to the loss of oxygen during heating, and to the appearance of electronic conductivity. Therefore, an air atmosphere is highly preferable for the LLTO sintering in order to avoid any oxygen loss and Ti^{4+} reduction.

Electrical conductivity measurements are carried out on pellets of ≈5 mm in diameter and ≈1.5 mm in thickness with ion blocking sputtered Pt electrodes under dehydrated N_2 atmosphere in a two-probe cell (DataLine). The Frequency Response Analyser (Solartron 1260) and the Dielectric Interface (Solartron 1296) are used in the frequency domain from 1 MHz to 1 Hz. The measurements are performed in the temperature range from RT to 400 °C by increasing and decreasing the temperature. Before any measurement, the linearity of the electrochemical system is checked and we found that it remains linear up to 2.0 V (rms), even at high temperature. Therefore, we used an ac voltage of 500 mV (rms) for all the temperatures investigated. Before each impedance measurements, a time of 45 min is necessary to obtain thermal equilibrium of the sample, after a step of 25 °C. The Zview software of Solartron (version 2.7), based on the LEVM software of J.R. Macdonald, is used to fit the experimental data. In all the analysis, the χ^2 value is ensured to be less than 5×10^{-4}. The overall resistivity of the samples is obtained from both the impedance diagrams, by taking the intercept of the low-frequency semicircle with the real axis, and the form factor of the sample. The form factor f ($f = l/s$ in cm^{-1}) is obtained from the geometric diameter, d with $s = \pi d^2/4$, and thickness, l, of the pellet.

Compactness of the pellet is determined from the ratio of experimental to theoretical density. The density of the pellet is determined from the accurate measurements of the sample volume and weight. The relative error on the density of the pellets is found to be 0.8%. The theoretical density is determined from the molecular weight of LLTO and the unit cell parameters ($a = b \approx c/2 = 3.874$ Å) as found in [18]. For $x = 0.10$, the theoretical density is $5.040 \pm 0.005\ g\,cm^{-3}$.

Microstructure observations are performed with a Hitachi 2300 scanning electron microscope (SEM).

3. Results

3.1. Dilatometry analysis

Sintering process is well known to be an efficient tool to influence the microstructure of a ceramic and hence to decrease the grain boundary resistance. However, the optimisation of the sintering temperature, time and atmosphere are necessary to get a desired microstructure. At the same time, it is necessary to avoid any undesirable effects, such as change of composition or lithium loss in these oxides, during the heating process. Dilatometry, is a versatile tool to study the sintering process and to determine the sintering temperature. Fig. 1 shows the dilatometry curve obtained on LLTO in open air atmosphere at a heating rate of 5 °C min^{-1}. This curve can be separated into three parts. The first one, from 100 °C to 900 °C, displays a small positive length change, which may be due to the thermal expansion of the sample. The second part, from 900 °C to 1300 °C, displays a strong decrease of the length, which is due to the shrinkage of the material during the sintering process. Finally the third one, above 1300 °C, does not display any change of the dimension of the sample. From this analysis, it can be concluded that sintering process of LLTO occurs in the temperature range from 900 °C to 1300 °C.

In order to study the effect of the sintering process on both the microstructure of LLTO and its electrical properties, isostatically pressed pellets of LLTO have been heat-treated at different temperatures. The selected temperatures are 600 °C and 800 °C, before sintering, 1000 °C, during sintering, and 1200 °C, at the final stage of the sintering. These points are marked as asterisks in Fig. 1. All the heating treatments have been carried out in open air for 2 h. To study the effect of the heating time we also heated a pressed pellet of LLTO at 1200 °C for 8 h. Therefore, we prepared five samples with different heating temperatures and times. The nomenclature of the pellets are LLTO-600C-2h, LLTO-800C-2H, LLTO-1000C-2H, LLTO-1200C-2H and LLTO-1200C-8H. During sintering, the volume of the pellet decreases and the compactness increases. The diameter and the compactness of the pellets as a function of the heat-treatment temperature are given in Table 1.

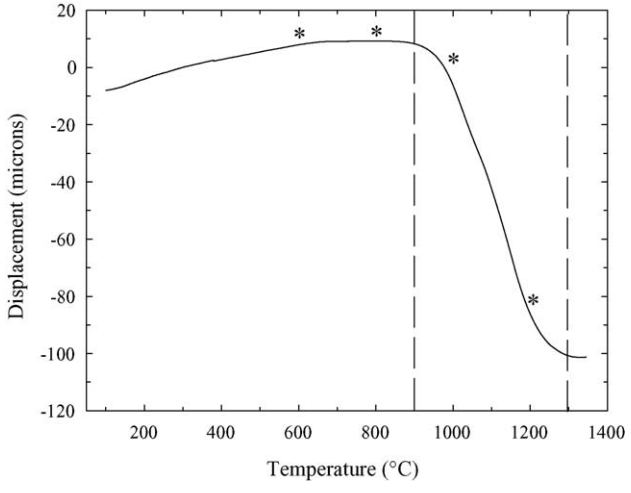

Fig. 1. Dilatometry curve of a pellet obtained by isostatically pressing $Li_{0.3}La_{0.56}TiO_3$ powder obtained by sol–gel method. Heating rate is 5 °C/min. The asterisks refer to the temperature at which the pellets have been further heat-treated for impedance investigation.

Table 1
Diameter, compactness and overall resistivity of the pellets of $Li_{0.3}La_{0.56}TiO_3$ as a function of the heating treatment temperature

Sample	Diameter (mm) ±0.01	Compactness (%) ±0.8	Overall resistivity ρ (ohm cm) at RT
600C-2H	5.05	64.4	2×10^8
800C-2H	5.06	67.8	1.5×10^8
1000C-2H	4.78	83.2	9×10^5
1200C-2H	4.50	97.7	3×10^4
1200C-8H	4.50	95.5	3×10^4

3.2. SEM analysis

Fig. 2(a–d), show the SEM images of the LLTO heat-treated in air at different temperatures and times. The SEM pictures of LLTO heated at 800 °C and 1000 °C (Fig. 2a and b) show a non-uniform microstructure which is due to the grain size distribution and agglomeration, as previously reported.[17] The agglomeration of the grains leads to the irregular grain shapes. However, sample sintered at 1000 °C shows the presence of more well-formed grains when compared to sample sintered at 800 °C. This may be due to the starting of the sintering process at 1000 °C as noted in the dilatometry curve analysis. The LLTO sintered at 1200 °C for 2 h (Fig. 2c) shows large grains with regular shape. The octahedral shape is well visible. This high grain size and regular shape is due to the sufficient temperature for sintering process as identified in dilatometry studies. LLTO sintered at 1200 °C for 8 h (Fig. 2d) provides more regular and higher grain size than LLTO sintered for 2 h. This is due to the longer sintering time and to the occurring of grain growth at the same time as sintering proceeds.

3.3. Impedance diagrams

Figs. 3–5 present three series of impedance spectra of LLTO pellets heated at different temperatures. The diagrams are plotted in the Nyquist plane. The first series (Fig. 3) is obtained with a pellet heat-treated at 800 °C for 2 h (before the sintering process takes place). Fig. 3a–d correspond to four impedance diagrams recorded at 20 °C, 280 °C, 400 °C and back to 37 °C, respectively. The second series (Fig. 4) is obtained with a pellet heat-treated at 1000 °C for 2 h (at the beginning of the sintering process). Fig. 4a–c correspond to three impedance diagrams recorded at 97 °C, 330 °C and back to 37 °C, respectively. The third one (Fig. 5) is obtained with a pellet heat-treated at 1200 °C for 2 h, which corresponds to the end of the sintering process. Fig. 5a–c correspond to three impedance diagrams recorded at 37 °C, 270 °C and back to 37 °C, respectively.

All the diagrams display one arc of circle which is related to the bulk and the grain boundary parts of the pellet and a straight line at low frequency which is related to the polarisation

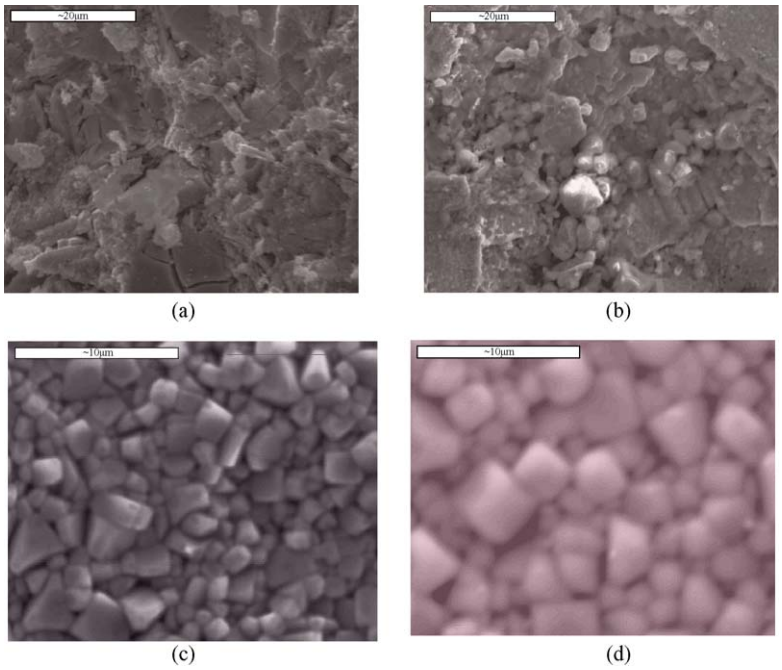

Fig. 2. SEM images of $Li_{0.3}La_{0.56}TiO_3$ heat-treated in air at different temperatures and times: (a) LLTO-800C-2H; (b) LLTO-1000C-2H; (c) LLTO-1200C-2H; (d) LLTO-1200C-8H.

of the electrodes. The diagrams obtained with non-sintered pellets (Fig. 3) are different from those obtained with sintered ones (Figs. 4 and 5) in two ways: the arc of circle is much more depressed and the frequency at which the electrode polarisation occurs is much lower. For non-sintered sample, the electrode polarisation does not appear at RT even at 1 Hz (Fig. 3d), although it occurs around 70 Hz when pellets are sintered (Figs. 4c and 5c). These observations suggest that before sintering, the entire diagram is totally dominated by the impedance of the grain boundaries, which is very high compared to the bulk impedance. We recall that LLTO is a fast purely ionic conductor with a bulk conductivity of 10^{-3} S cm^{-1} at RT,[19] therefore the bulk impedance is very small at this temperature. The RT overall resistivity ($\rho = R\,s/l$) of the samples is reported in Table 1. The high overall resistivity of the pellet observed before sintering is due to the high grain boundary resistance which arises from the polycrystalline nature of the material with irregular shape, as shown in Fig. 2a, grain size distribution and the presence of many pores since the compactness is low, i.e. $67.8 \pm 0.8\%$. As sintering occurs, the overall resistivity decreases of several orders of magnitude, the grain size increases and the compactness also increases to reach $97.7 \pm 0.8\%$ at 1200 °C. It is interesting to note that, the overall resistivity of the samples does not change with the sintering time from 2 h to 8 h at 1200 °C. Therefore, for a practical application, a short sintering time will be preferred since it will reduce the grain boundary resistance and avoid lithium loss.

To analyse the impedance data, electrical equivalent circuits made of series RC elements have been used. As shown by Fleig et al.,[8] a series model is preferred to a parallel one since it enables a simple interpretation or estimation of the elements. However, to take into account the fact that the semicircles are not centred on the real axis, we used constant phase element (CPE) instead of pure capacitance C. In Figs. 3–5 and for each impedance diagram, the experimental data are shown as open circles, the electrical equivalent circuit used to fit the impedance diagram (when possible) is shown at the right side of the diagram and the result of the fitting procedure as a line.

According to the simple BLM, only two serial (R,CPE) elements are generally necessary to fit the impedance diagrams, one being related to the bulk and the other to the grain boundary of the material.[5–8] The electrode polarisation at low frequency can be modelised by a CPE. Such a simple model perfectly applies for the pellets sintered at 1200 °C for 2 or 8 h, in the whole temperature range investigated for the impedance data recording, from RT to 400 °C. Because the time constants of these two relaxations are not highly different, they do not appear as two distinct semicircles in the impedance diagram. This is shown in Fig. 5a. Furthermore, when temperature increases, the resistance of the bulk decreases and the CPE remains almost constant. As a consequence, the $(R,CPE)_{bulk}$ element transforms to only R_{bulk} as shown in Fig. 5b. On the other hand, the impedance spectra of the pellet heated at 600, 800 and 1000 °C for 2 h cannot be fitted with such a simple model. For the pellet heated at 1000 °C for 2 h (Fig. 4), the bulk relaxation is visible at high frequency and a low-frequency semicircle is observed followed by the electrode polarisation at lower frequencies. The low-frequency semicircle, which corresponds to the relaxation into the grain boundaries, is much more difficult to fit and to interpret. Indeed, when temperature increases, from RT to around 200 °C, this semicircle can be fitted with two (R,CPE) elements (Fig. 4a). Above 200 and up to 400 °C, only one (R,CPE) element is sufficient (Fig. 4b). When temperature decreases from 400 °C to 200 °C one (R,CPE) element is used but below 200 °C two serial (R,CPE) elements

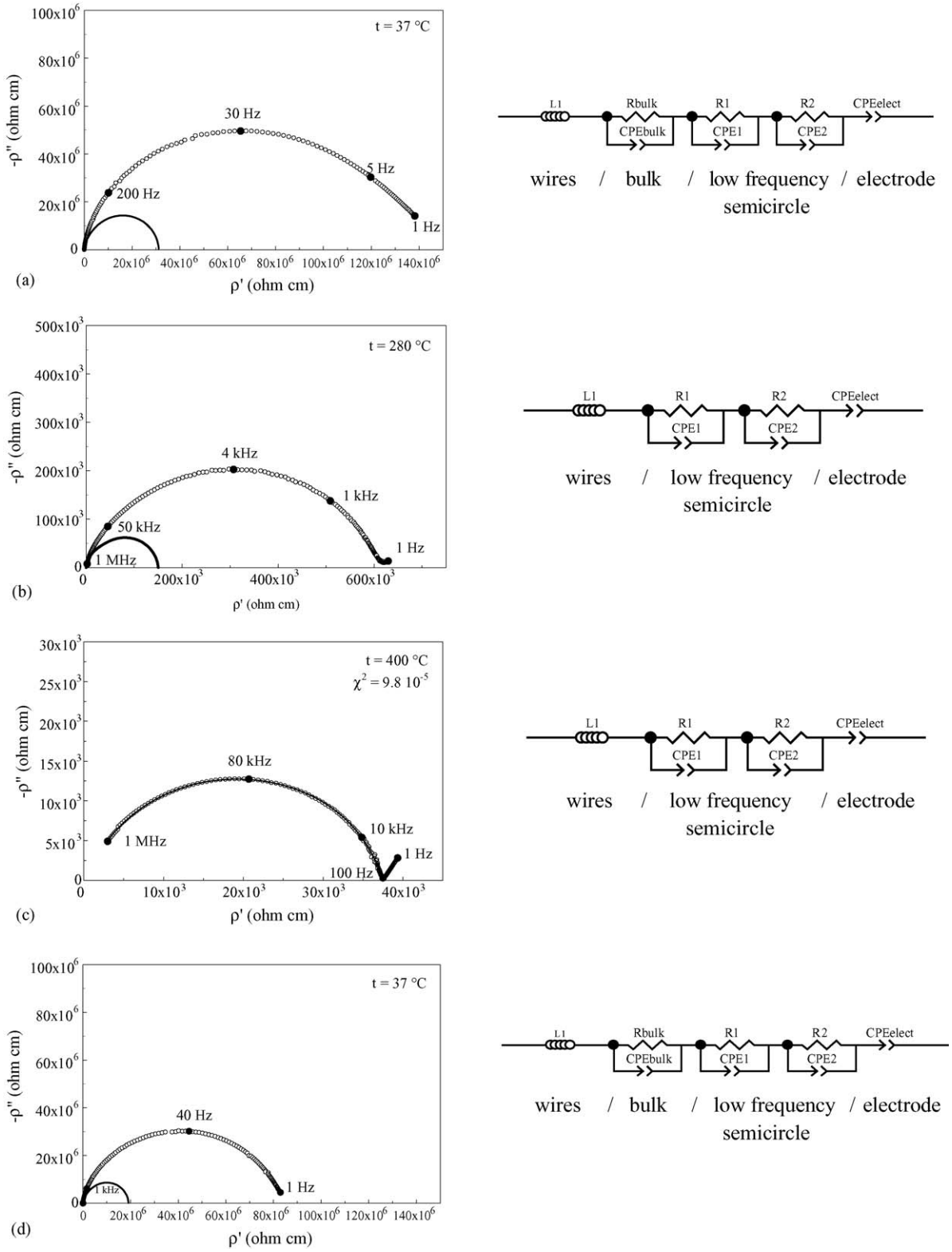

Fig. 3. Impedance diagrams recorded at (a) 20 °C, (b) 280 °C, (c) 400 °C and (d) 37 °C (ac voltage of 500 mV rms). The pellet of $Li_{0.3}La_{0.56}TiO_3$ has been heat-treated at 800 °C for 2 h. (o) refers to the experimental data and (- - -) to the fitting curve obtained from the corresponding electrical model shown on the right side of the diagram.

are necessary (Fig. 4c). This result shows that for the low frequency semicircle one relaxation disappears when temperature increases above 200 °C and appears again when temperature decreases below this temperature.

For the pellets heated at 600 and 800 °C, the impedance diagrams are dominated by grain boundaries resistance, therefore the bulk resistance cannot be determined with great accuracy. As shown in Fig. 3, the impedance diagrams are made of only

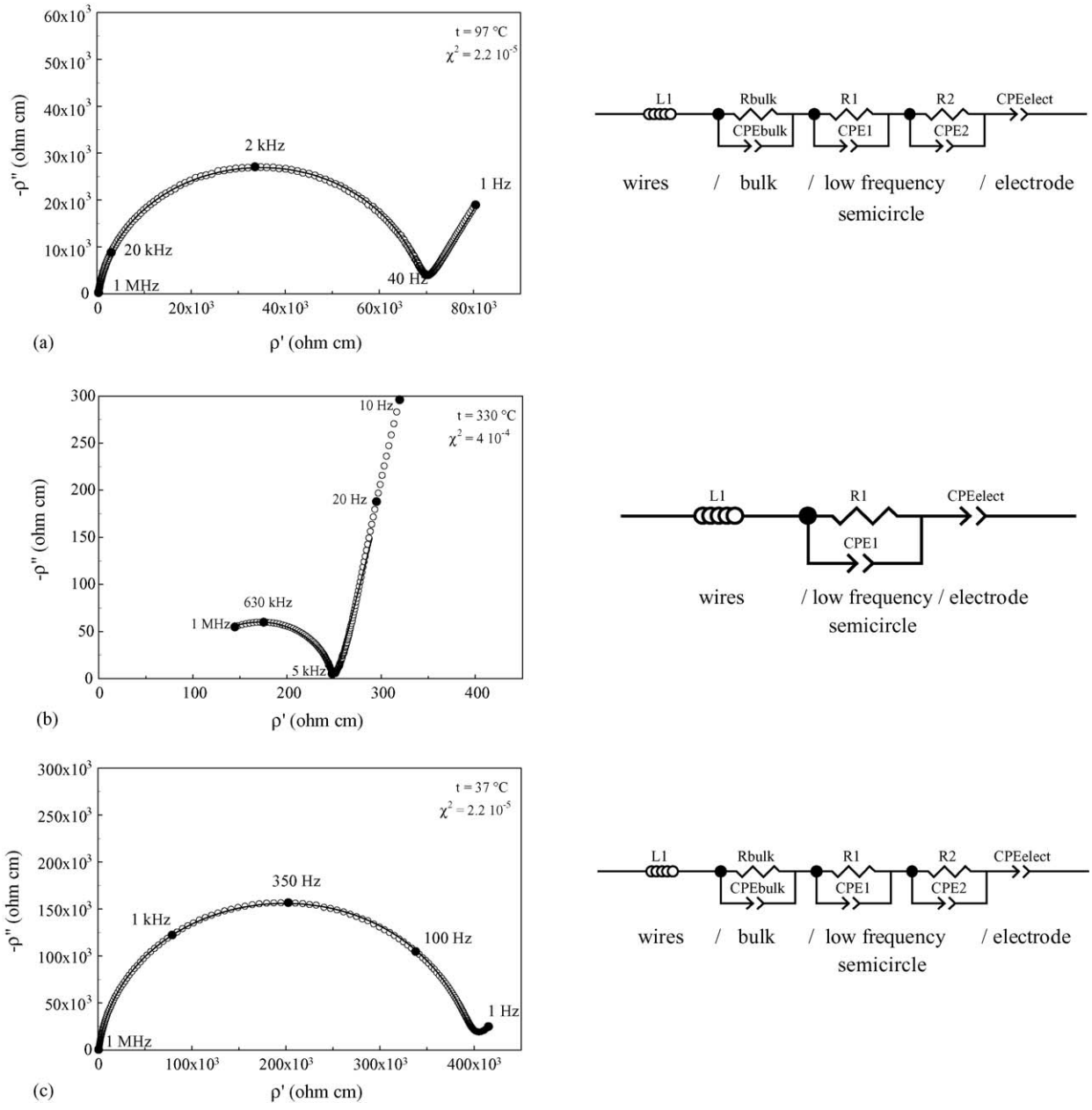

Fig. 4. Impedance diagrams recorded at (a) 97 °C, (b) 330 °C and (c) 37 °C (ac voltage of 500 mV rms). The pellet of $Li_{0.3}La_{0.56}TiO_3$ has been heat-treated at 1000 °C for 2 h. (o) refers to the experimental data and (- - -) to the fitting curve obtained from the corresponding electrical model shown on the right side of the diagram.

one semicircle that covers the whole frequency range investigated, i.e. 1 MHz–1 Hz. This semicircle shows a very complex shape that cannot be easily fitted and that changes with recording impedance diagram temperature. An electrical equivalent circuit made of two (R,CPE) elements in series to take into account the relaxation into the grain boundaries has been used, and the impedance diagram has been simulated as shown as a line. It can be seen that a large difference exists between the simulated plot and the experimental one below 300 °C. On the other hand, at higher temperature this model perfectly fits the experimental data (Fig. 4c). This particular "fish" shape arises from the different grain size and agglomerates, which are present in the material. We already reported, in a previous paper,[17] the existence of different grain sizes and agglomerates in LLTO prepared by the sol–gel method. This is also shown in the MEB pictures of Fig. 2, as well as in the histogram shown in Fig. 6 which reveals three types of particles and agglomerates of ≈200 nm, 5 μm and 100 μm size.

According to the electrical equivalent circuits proposed, it is possible to determine the values of the different resistance that we call R_{bulk} for the high frequency one (when it is possible to determine it with good accuracy), R_1 and R_2 for the different (R,CPE) elements of the low-frequency semicircle. Fig. 7 presents the bulk conductivity, σ_{bulk}, of the different samples plotted in an Arrhenius fashion. σ_{bulk} is calculated according to the relationship: $\sigma_{bulk} = f/R_{bulk}$, where f is the form factor of the sample. The bulk conductivity and its activation energy ($E_a \approx 0.25 \pm 0.02$ eV) are found to be almost constant. We found

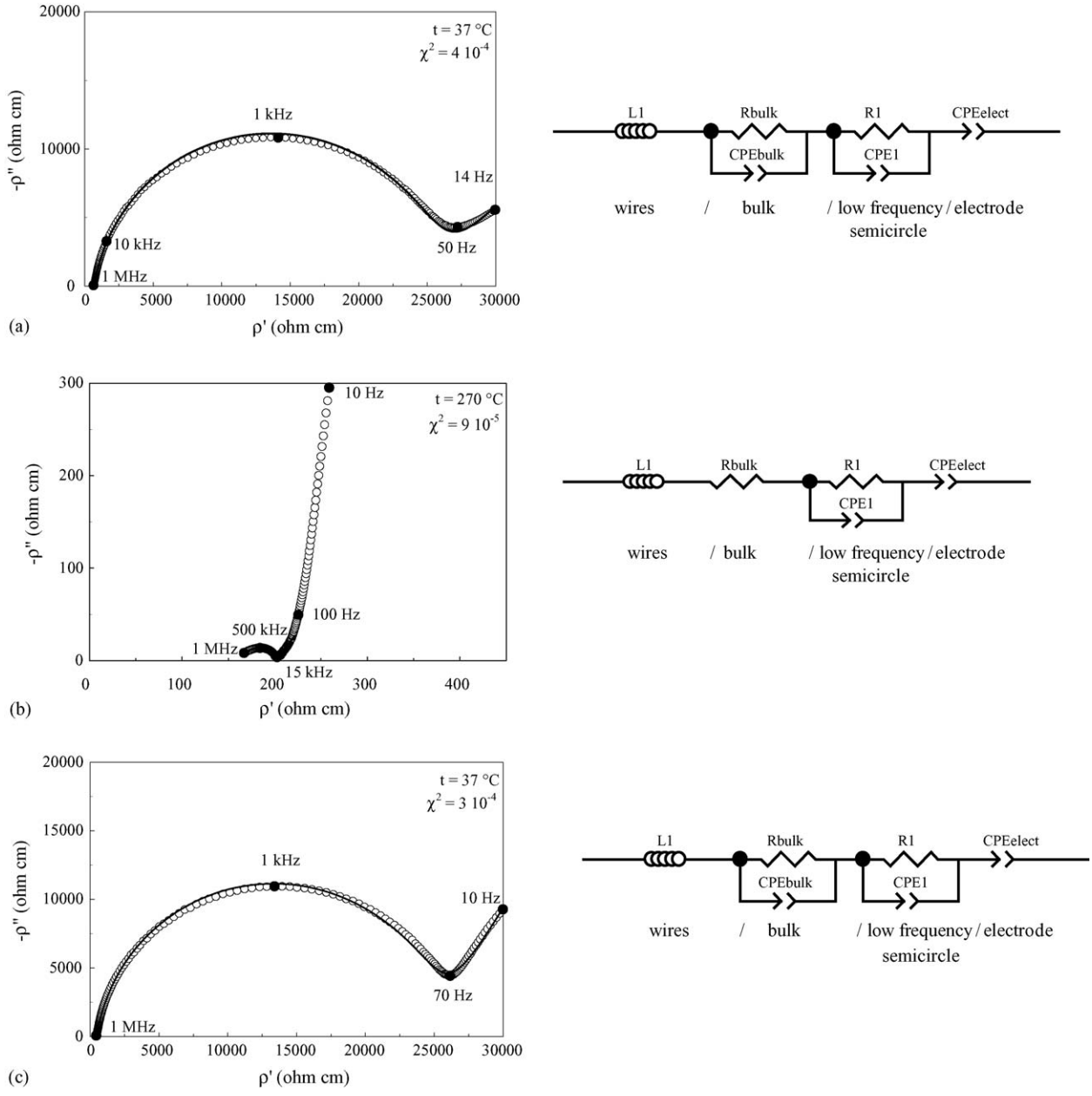

Fig. 5. Impedance diagrams recorded at (a) 37 °C, (b) 270 °C and (c) 37 °C (ac voltage of 500 mV rms). The pellet of $Li_{0.3}La_{0.56}TiO_3$ has been heat-treated at 1200 °C for 2 h. (o) refers to the experimental data and (- - -) to the fitting curve obtained from the corresponding electrical model shown on the right side of the diagram.

that they do not change with sintering temperature and time suggesting that the crystal structure of the oxide does not change with the sintering process. This result is in good agreement with the previous results obtained by Kim et al. [20] who reported a very small increase of bulk conductivity with sintering time despite a large microstructure change. Recently, Ban et al. [21] reported an increase of LLTO bulk conductivity, greater than one order of magnitude, when sintering temperature increases from 1100 °C to 1200 °C. They explained that this increase was due to the change in the lattice parameters of the oxide, which arises from a Li loss during sintering. This explanation does not agree with the results of Inaguma et al.[19] and Bohnké et al.[22] who reported only small change in the bulk conductivity with the oxide lithium content. Since sintering process alters only the microstructure of LLTO and does not change its crystal structure, as confirmed by X-ray diffraction analysis,[18] a constant bulk conductivity is expected over different sintering temperature and time. This is observed in this work. This result also validates the goodness of our electrical models.

Fig. 8a shows the variation of the conductance of the bulk and the grain boundaries as a function of temperature for the pellet heat-treated at 1200 °C for 2 h. These results are plotted in an Arrhenius fashion, i.e. $\lg(G \times T)$ as a function of $1000/T$. G represents the conductance, or the inverse of the resistance R, determined by using the electrical model shown in Fig. 5. Because the thickness of the grain boundary is unknown, only the conductance of the grain boundaries can be determined. Their conductivity cannot be obtained. The activation

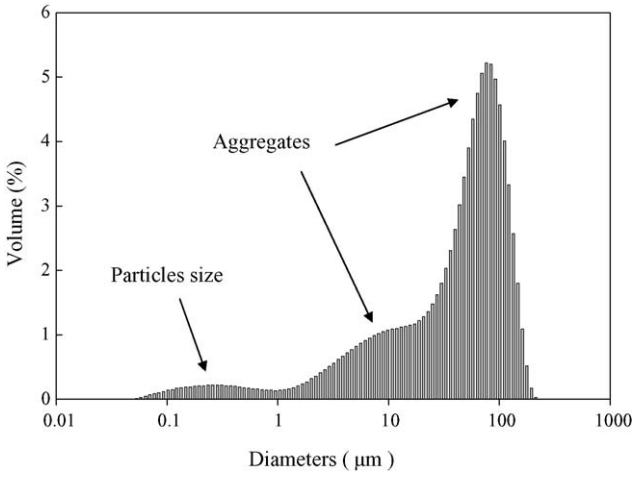

Fig. 6. Histogram of the particles and aggregates size of $Li_{0.3}La_{0.56}TiO_3$ sample prepared by a modified Pechini-type polymerizable precursor technique after heating at 900 °C for 2 h from [17].

energies of the bulk and grain boundary relaxation are 0.24 eV and 0.38 eV, respectively. For the pellet heat-treated at 1200 °C for 8 h, the activation energies of the bulk and the grain boundary are 0.27 eV and 0.32 eV, respectively. Fig. 8b shows the variation of the corresponding relaxation time of the grain boundary relaxation as a function of temperature, plotted in an Arrhenius fashion. The relaxation characteristic time, t_{relax}, is obtained from the determination of the characteristic frequency, f_{relax}, of the (R,CPE) relaxation. We recall that $t_{relax} = 1/(2\pi f_{relax})$. The characteristic time follows the Arrhenius law in the whole temperature range investigated. The activation energy is 0.42 eV,

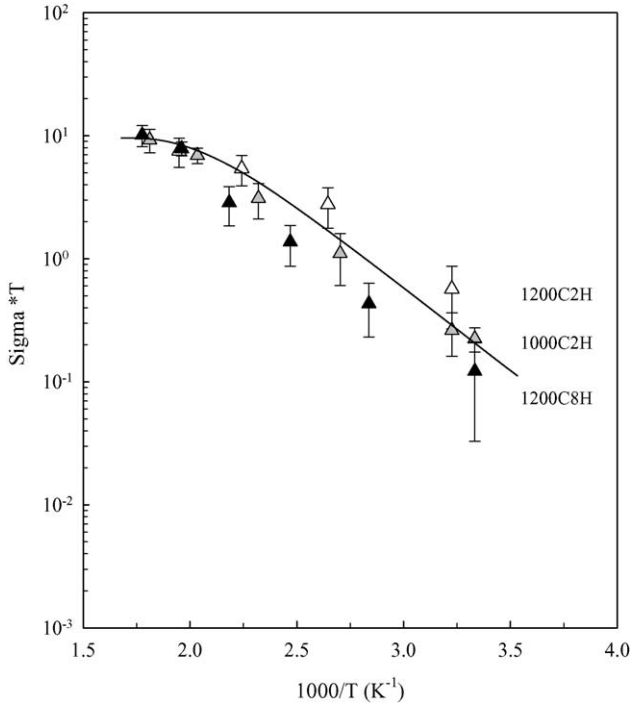

Fig. 7. Bulk conductivity as a function of temperature (plotted in an Arrhenius fashion) for the heat-treated LLTO pellets.

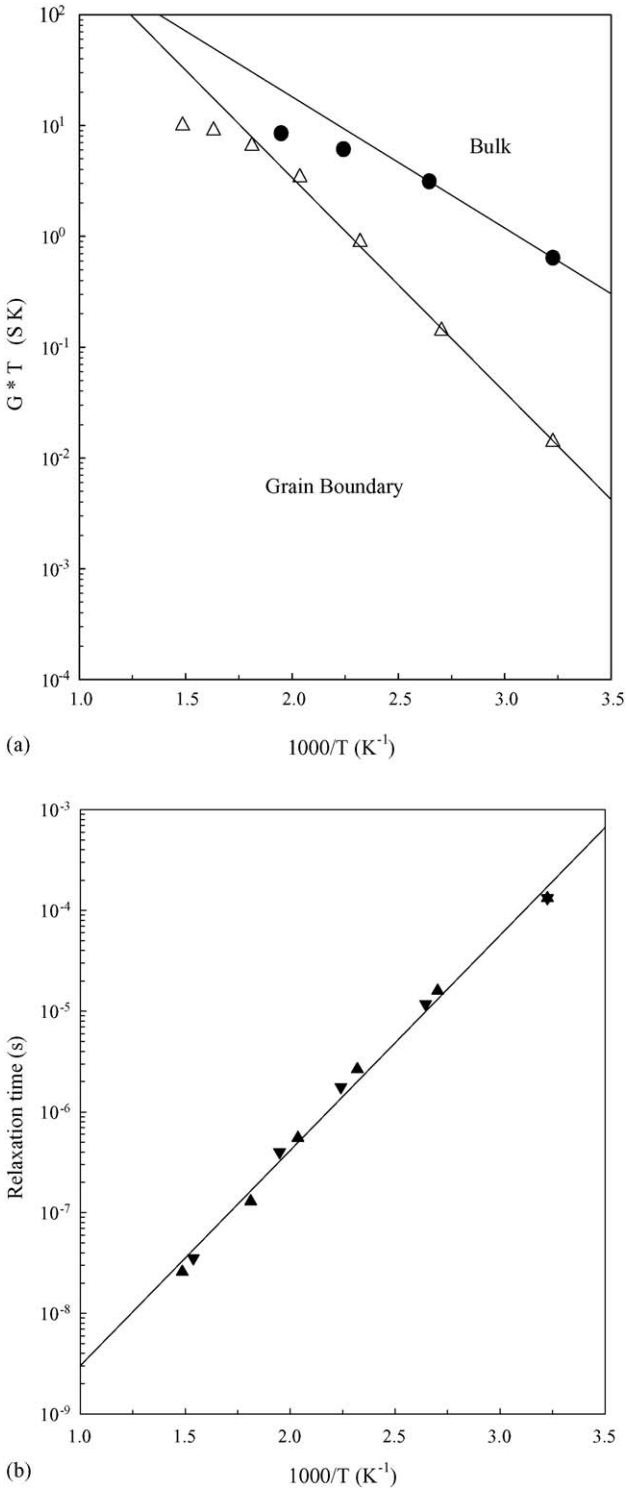

Fig. 8. LLTO pellet heat-treated at 1200 °C for 2 h ($f = 0.89\,cm^{-1}$): (a) conductance of the bulk and grain boundary as a function of temperature; (b) characteristic time of the grain boundary relaxation as a function of time. All the curves are plotted in an Arrhenius fashion.

close to the activation energy of the grain boundary conductance determined previously.

Fig. 9a presents the conductance of the bulk and the grain boundaries as a function of temperature for the pellet heat-treated at 1000 °C for 2 h. The two grain boundaries conductances refer

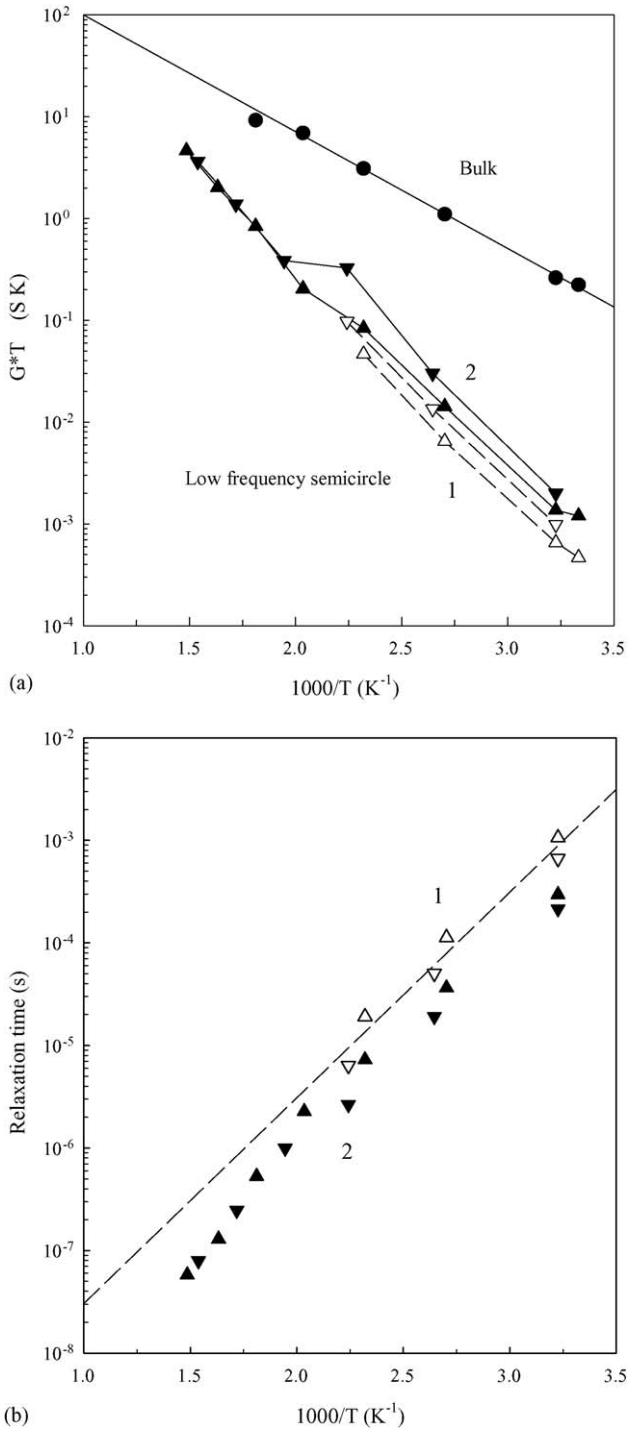

Fig. 9. LLTO pellet heat-treated at 1000 °C for 2 h (f = 0.83 cm^{-1}): (a) conductance of the bulk and grain boundary as a function of temperature; (b) characteristic time of the two grain boundary relaxations as a function of time. All the curves are plotted in an Arrhenius fashion.

to the resistances of the two (R,CPE) elements shown in Fig. 4. The disappearance of one (R,CPE) element is shown in this figure when temperature reaches a value greater than 200 °C. The activation energies of the bulk and the grain boundaries (high- and low-frequency relaxations) are 0.23 eV, 0.37 eV and 0.39 eV, respectively. Fig. 9b shows the variation of the corresponding characteristic times of the two (R,CPE) relaxations. It shows the disappearance of the slowest relaxation when temperature increases.

4. Discussion

In the present study, it is shown that the low-frequency semicircle of the impedance spectra, which corresponds to the electrical grain boundaries behaviour of the material, changes significantly with the compactness and the microstructure of the pellet. For non-sintered materials, with porosity and grain size distribution with high resistive grain boundary, this low-frequency semicircle shows a very complex shape that cannot be easily fitted. On the other hand, as soon as sintering is effective, the compactness of the oxide increases, the grain size increases and the grain shape becomes regular. Therefore, the grain boundary semicircle can be fitted with only one (R,CPE) element whatever the impedance diagram recording temperature, as shown for the 1200C-2H and 1200C-8H samples. Finally, for pellets heat-treated at intermediate temperature, i.e. 1000 °C, the low-frequency semicircle can be fitted with either one or two (R,CPE) elements depending on the impedance diagram recording temperature, i.e. when temperature increases, one (R,CPE) element vanishes and appears again as soon as temperature decreases. The reversibility of this phenomenon clearly means that the microstructure of the oxide does not change with temperature. Therefore, the question that arises is why some grain boundary, even present in the material, cannot be seen by the IS?

In a series of recent papers,[8–13] Fleig et al. have clearly shown, by numerical calculations, that when a ceramic, with low-conducting grain boundaries, shows a broad grain size distribution or if the distribution of grain size is spatially inhomogeneous, its impedance can deviate from the one derived from the BLM. The BLM refers to an ideal microstructure. It assumes regular, exactly cubic, isotropic grains of the same size, straight contacts between the grains and uniform grain boundary properties. In such an ideal microstructure, the potential distribution is perfectly homogeneous, and then the current flow is perpendicular to the electrodes. A simple equivalent circuit made of two serial (R,CPE) elements can be used to fit the impedance data: one (R,CPE) element can be related to the bulk of the material and the other one to the grain boundary enabling the determination of the bulk and grain boundary conductance. However, a grain size distribution or the agglomeration of grains as well as the presence of pores that represent low conducting boundaries can cause deviations from the BLM as well as a change in the shape of the low-frequency impedance spectra. Deviations would then be caused by the "detours effect", which means that current detours around blocking grain boundaries or pores occur if this lowers the impedance. As a consequence of these current detours, an inhomogeneous current distribution appears in the material. It has to be pointed out that the conductivity of the grain interior (bulk conductivity) influences the "detours effect": detours will be easy in high bulk conductivity and therefore, low conducting grain boundaries will be avoided, on the other hand, detours will be difficult for low bulk conductivity. Therefore,

the size and the shape of the low-frequency semicircle of the impedance spectrum, which is generally associated to grain boundary impedance, can be influenced by the bulk conductivity. This means that for a given microstructure, if impedance spectra are taken at different temperatures, the increase of the bulk conductivity with temperature (that follows the Arrhenius law) may increase the proportion of current detours in the material and therefore can affect the low-frequency semicircle.

Another important point shown by Fleig is that the current distribution is frequency-dependent. So, an inhomogeneous current distribution, due to "detours effect", is observed only at low frequency, while a homogeneous current distribution results for frequencies of the order of the relaxation frequency of the bulk or higher. Indeed, at these very high frequencies, the grain boundaries are nearly dielectrically short-circuited. As a consequence, the high-frequency semicircle does not depend on the microstructure of the ceramic, and then on the sintering process, and reveals, in any case, the real bulk resistance or capacitance of the material.

These two features are of great importance when analysing the impedance spectra of the fast ionic conductor LLTO ceramic as a function of recording temperature. If it has been shown by Fleig that the homogeneity of the current distribution is frequency-dependent, this work clearly shows that it is also temperature-dependent. Apart from the fact that, for a given material, the bulk and grain boundary conductivity vary with temperature (according to the Arrhenius law), the temperature can also affect the current distribution by changing the proportion of current detours. As soon as "detours effect" is important, the low-frequency semicircle and the associated (R,CPE) elements cannot be interpreted in terms of resistance and capacitance of the grain boundary alone. Therefore, grain boundary conductance as well as relaxation times can deviate from the Arrhenius law.

It is what is observed for the ceramics heated at 1000 °C and in a more extend for the ceramics heated at 800 °C that show very inhomogeneous grain sizes, different high resistive grain boundaries, high porosity and consequently a "fish" shape impedance plot that varies with temperature.

For the ceramic heated at 1000 °C, the temperature dependence of the impedance spectra can be explained as follow. At low temperature, the current passes through the grains and for a great proportion through all the grain boundaries independently of their conductivity (Fig. 10a). Current detours are not very important. Two kinds of grain boundaries, with different conductance and relaxation characteristic time, can be distinguished, leading to two (R,CPE) elements (Fig. 9a and b). When temperature increases, the bulk conductivity increases as shown in Fig. 9, one (R,CPE) element disappears due to the current detours. The current tends to avoid the highest resistive grain boundary (Fig. 10b), that corresponds to the slowest relaxation, and then this grain boundary impedance cannot be observed on the impedance spectrum. Furthermore, the resistance and the relaxation time of the observed (R,CPE) element is affected by this current detour and their variation with temperature deviates from the Arrhenius law, as shown in Fig. 9a and b. These new pathways lead to slightly decrease the conductance and

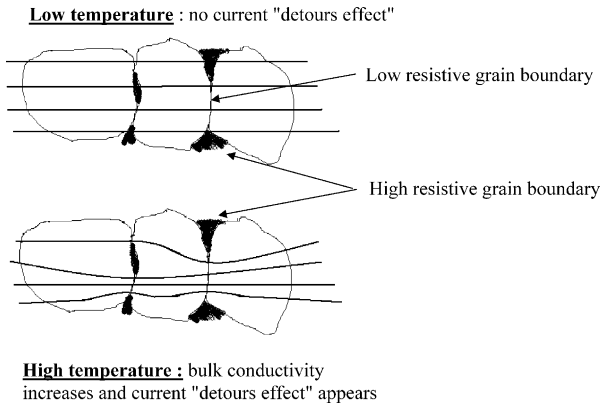

Fig. 10. Schematic diagram of the ceramic microstructure showing the low and high resistive grain boundaries. The diagram represents the ceramic after heat-treatment at 1000 °C for 2 h with the two grain boundaries regions. The lines represent the current flowing through the oxide under the applied potential and the appearance of current "detours effect" as temperature increases. At high temperature, the high resistive grain boundary is no more observed by impedance spectroscopy.

to increase the apparent activation energy. Finally, when temperature decreases again, the current detours will be less and less important and then the second (R,CPE) element appears again.

The same behaviour can be observed for the ceramic heated at 800 °C. However, the microstructure of this pellet is more complex than the microstructure of the previous sample. Fig. 6 shows the presence of three kinds of grain and agglomerates leading to three kinds of grain boundaries. Furthermore, porosity is important leading to the presence of insulating pores in addition to grain/grain boundaries and to two kinds of agglomerates/agglomerates boundaries. Such a complex microstructure leads to a very complex three-dimensional (*R*,*C*) network that gives a "fish" shape impedance Nyquist diagram which cannot be analysed with a one-dimensional (or series) equivalent electrical circuit. The shape of the low-frequency semicircle is probably due to the current detours effect.

5. Conclusion

The IS data obtained from fast ionic conductor ceramics, $Li_{3x}La_{2/3-x}TiO_3$ with random microstructure and porosity, display a complex low-frequency semicircle. When sintering is effective, the ceramic has very low porosity and low resistive grain boundary, consequently the low-frequency semicircle is fitted with only one (R,CPE) element that corresponds to the grain boundary relaxation. On the other hand, when the ceramic has a low compactness and/or a distribution of grain sizes with high resistive grain boundary, the temperature dependence of the low-frequency semicircle reveals the presence of "detours effect" in the material as temperature increases. "Detours effect" means that current detours around blocking grain boundary and/or insulating pores occur if this effect lowers the impedance. This effect leads to the disappearance of the slowest (R,CPE) relaxation when temperature increases and its recovery when temperature decreases.

Acknowledgment

M. Vijayakumar thanks the "Région des Pays de la Loire" for financial support through a postdostoral fellowship.

References

1. In *Impedance Spectroscopy—Emphasizing Solid Materials and Systems*, ed. J.R. Macdonald. John Wiley and Sons, New York, 1987.
2. In *A treatise on Electricity and Magnetism*, ed. J.C. Maxwell *(2nd ed.)*. Clarendon Press, Oxford, 1881.
3. Bauerle, J. E., *J. Phys. Chem. Solids*, 1969, **30**, 2657.
4. Beekmans, N. M. and Heyne, L., *Electrochim. Acta*, 1976, **21**, 303.
5. Badwal, S. P. S., *Solid State Ionics*, 1995, **76**, 67.
6. Steil, M. C., Thevenot, F. and Kleitz, M., *J. Electrochem. Soc.*, 1997, **144**, 390.
7. Christie, G. M. and Van Verkel, F. P. F., *Solid State Ionics*, 1996, **83**, 17.
8. Fleig, J. and Maier, J., *J. Electroceram.*, 1997, **1**, 73.
9. Fleig, J., Pham, P. and Sztulzaft, P., *J. Mater. Solid State Ionics*, 1998, **113–115**, 739.
10. Fleig, J. and Maier, J., *J. Electrochem. Soc.*, 1998, **145**(6), 2081.
11. Fleig, J. and Maier, J., *J. Am. Ceram. Soc.*, 1999, **82**(12), 3485.
12. Fleig, J., *Solid State Ionics*, 2000, **131**, 117.
13. Fleig, J., *Solid State Ionics*, 2002, **150**, 181.
14. Bohnké, C., Bohnké, O., Duroy, H. and Fourquet, J-L., French Patent No. 0210730 (29/08/2002).
15. Bohnké, C., Duroy, H. and Fourquet, J.-L., *Sens. Actuators B, Chem.*, 2003, **89**(3), 240.
16. Bohnké, C. and Fourquet, J.-L., *Electrochim. Acta*, 2003, **48**, 1869.
17. Vijayakumar, M., Inaguma, Y., Mashiko, W., Crosnier-Lopez, M.-P. and Bohnké, C., *Chem. Mater.*, 2004, **16**, 2719.
18. Fourquet, J.-L., Duroy, H. and Crosnier-Lopez, M.-P., *J. Solid State Chem.*, 1996, **127**, 283.
19. Inaguma, Y., Liquan, C., Itoh, M., Nakamura, T., Uchida, T., Ikuta, H. *et al.*, *Solid State Commun.*, 1993, **86**, 689.
20. Kim, J.-G., Kim, H.-G. and Chung, H.-T., *J. Mater. Sci. Lett.*, 1999, **18**, 493.
21. Ban, C. W. and Choi, G. M., *Solid State Ionics*, 2001, **140**, 285.
22. Bohnké, O., Emery, J., Fourquet, J.-L. and Badot, J.-C., In *Recent Research Development in Solid State Ionics*, *Vol 1*, ed. S.G. Pandalai. Transworld Research Network Publishers, Trivandrum, 2003, p. 47.